Inorg. Chem. **2005**, *44*, 6456–6462

Inorganic Chemistry
Article

Heterovalent Au^{III}–M^{I} (M = Cu, Ag, Au) Complexes Derived from Incorporation of $[Au(tdt)_2]^-$ (tdt = Toluene-3,4-dithiolate) with $[M_2(dppm)_2]^{2+}$ (dppm = Bis(diphenylphosphino)methane)

Yan-Dan Chen,[†] Li-Yi Zhang,[†] Yong-Hai Qin,[†] and Zhong-Ning Chen*,[†,‡]

State Key Laboratory of Structural Chemistry, Fujian Institute of Research on the Structure of Matter, The Chinese Academy of Sciences, Fuzhou, Fujian 350002, China, and State Key Laboratory of Coordination Chemistry, Nanjing University, Nanjing 210093, China

Received April 7, 2005

Polynuclear heterovalent Au^{III}–M^{I} (M = Cu, Ag, Au) cluster complexes $[Au^{III}Cu^{I}_8(\mu\text{-dppm})_3(tdt)_5]^+$ (**1**), $[Au^{III}_3Ag^{I}_8(\mu\text{-dppm})_4(tdt)_8]^+$ (**2**), and $[Au^{III}Au^{I}_4(\mu\text{-dppm})_4(tdt)_2]^{3+}$ (**3**) were prepared by reaction of $[Au^{III}(tdt)_2]^-$ (tdt = toluene-3,4-dithiolate) with 2 equiv of $[M^{I}_2(dppm)_2]^{2+}$ (dppm = bis(diphenylphosphino)methane). Complex **3** originates from incorporation of one $[Au^{III}(tdt)_2]^-$ with two $[Au^{I}_2(dppm)_2]^{2+}$ components through Au^{III}–S–Au^{I} linkages. Formation of complexes **1** and **2**, however, involves rupture of metal–ligand bonds in the metal components and recombination between the ligands and the metal atoms. The $Au(tdt)_2$ component connects to four M^{I} atoms through Au^{III}–S–M^{I} linkages in syn and anti conformations in complexes **1** (M = Cu) and **3** (M = Au), respectively, but in both syn and anti conformations in complex **2** (M = Ag). The tdt ligand exhibits five types of bonding modes in complexes **1**–**3**, chelating Au^{III} or M^{I} atoms as well as bridging Au^{III}–M^{I} or M^{I}–M^{I} atoms in different orientations. Although complexes **1** and **2** are nonemissive, $Au^{III}Au^{I}_4$ complex **3** shows room-temperature luminescence with emission maximum at 555 nm (τ_{em} = 3.1 μs) in the solid state and at 570 nm (τ_{em} = 1.5 μs) in acetonitrile solution.

Introduction

Gold chemistry has attracted a great deal of attention in the past two decades.[1−5] One of the most intriguing features in gold complexes is the tendency to display metal−metal interactions, whose energy is comparable with that of hydrogen bonds.[1] The presence of thiolates or/and phosphines usually favors formation of ligand-bridged or -unsupported gold clusters through gold−gold contacts.[6,7] It has been demonstrated that intra- and/or intermolecular gold−gold interactions frequently induce intriguing optoelectronic properties[8−10] and play a key role in medical applications.[11] Nevertheless, relative to numerous monovalent or homonuclear Au^{I} and Au^{III} complexes,[1−13] heterovalent (Au^{III}−Au^{I})[14−34] or heteronuclear (Au^{III}−Ag^{I} and Au^{III}−Cu^{I})[35−39]

---

* To whom correspondence should be addressed. E-mail: czn@fjirsm.ac.cn.

[†] The Chinese Academy of Sciences.

[‡] Nanjing University.

(1) Pyykkö, P. *Chem. Rev.* **1997**, *97*, 597.
(2) Schmidbaur, H. *Chem. Soc. Rev.* **1995**, 391.
(3) Fackler, J. P., Jr. *Inorg. Chem.* **2002**, *41*, 6959.
(4) Puddephatt, R. J. *Chem. Commun.* **1998**, 1055.
(5) Bardaji, M.; Laguna, A. *J. Chem. Educ.* **1999**, *76*, 201.
(6) Forward, J. M.; Bohmann, D.; Fackler, J. P., Jr.; Staples, R. J. *Inorg. Chem.* **1995**, *34*, 6330.
(7) Jones, W. B.; Yuan, J.; Narayanaswamy, R.; Young, M. A.; Elder, R. C.; Bruce, A. E.; Bruce, M. R. M. *Inorg. Chem.* **1995**, *34*, 1996.
(8) Wang, S.; Garzon, G.; King, C.; Wang, J. C.; Fackler, J. P., Jr. *Inorg. Chem.* **1989**, *28*, 4623.
(9) Xiao, H.; Weng, Y.-X.; Wong, W.-T. Wong, Mak, T. C. W.; Che, C.-M. *J. Chem. Soc., Dalton Trans.* **1997**, 221.
(10) Yam, V. W.-W.; Lai, T.-F.; Che, C.-M. *J. Chem. Soc., Dalton Trans.* **1990**, 3747.
(11) Shaw, C. F., III. *Chem. Rev.* **1999**, *99*, 2589.
(12) Mansour, M. A.; Lachicotte, R. J.; Gysling, H. J.; Eisenberg, R. *Inorg. Chem.* **1998**, *37*, 4625.
(13) Gimeno, M. C.; Laguna, A. *Chem. Rev.* **1997**, *97*, 511.
(14) Mèndez, L. A.; Jimènez, J.; Cerrada, E.; Mohr, F.; Laguna, M. *J. Am. Chem. Soc.* **2005**, *127*, 852.
(15) Canales, S.; Crespo, O.; Gimeno, M. C.; Jones, P. G.; Laguna, A. *Inorg. Chem.* **2004**, *43*, 7234.
(16) Fernández, E. J.; Gil, M.; Olmos, M. E.; Crespo, O.; Laguna, A.; Jones, P. G. *Inrog. Chem.* **2001**, *40*, 3018.
(17) Canales, S.; Crespo, O.; Gimeno, M. C.; Jones, P. G.; Laguna, A.; Mendizabal, F. *Organometallics* **2001**, *20*, 4812.
(18) Bardaji, M.; Laguna, A.; Orera, V. M.; Villacampa, M. D. *Inorg. Chem.* **1998**, *37*, 5125.
(19) Calhorda, M. J.; Canales, F.; Gimeno, M. C.; Jimènez, J.; Jones, P. G.; Laguna, A.; Veiros, L. F. *Organometallics* **1997**, *16*, 3837.
(20) Canales, F.; Gimeno, M. C.; Laguna, A. *Organometallics* **1996**, *15*, 3412.
(21) Laguna, A.; Laguna, M. *J. Organomet. Chem.* **1990**, *394*, 743.
(22) Fernández, E. J.; Gimeno, M. C.; Jones, P. G.; Laguna, A.; Laguna, M.; López-de-Luzuriaga, J. M. *J. Chem. Soc., Dalton Trans.* **1992**, 3365.

10.1021/ic050542n CCC: $30.25

chemistry is still in its infancy because of difficulty in controlling the heterovalent or heteronuclear assembly.

To attain luminescent materials, we have been interested in designing d^8-d^{10} or $d^{10}-d^{10}$ heterovalent or heteronuclear complexes by reaction of two types of metal components capable of incorporation to each other. A series of $Pt^{II}-M^{I}$ and $M^{I}-M'^{I}$ (M and M′ = Cu, Ag, or Au) heteronuclear complexes displaying rich photoluminescence with manifold emission origins have been prepared by combination of Pt(diimine)(dithiolate) or coinage metal alkynyl components with $[M'_2(dppm)_2]^{2+}$.[40−43] To promote this work, investigation of other new d^8-d^{10} heterovalent or heteronuclear assemblies has been pursued in our laboratory.

In view of the potentially bridging character and versatile bonding modes of the sulfur donors in $[Au(tdt)_2]^-$, it can serve as a useful precursor for design of $Au^{III}-M^{I}$ heterovalent or heteronuclear complexes with novel structural topology by incorporation with M^{I} components that can afford vacant or substitutable coordination sites. Thus, reactions of $[Au^{III}(tdt)_2]^-$ with $[M_2(dppm)_2]^{2+}$ (dppm = bis(diphenylphosphino)methane) were investigated, affording $Au^{III}Cu^{I}_8$, $Au^{III}_3Ag^{I}_8$, and $Au^{III}Au^{I}_4$ complexes when M = Cu^{I}, Ag^{I}, and Au^{I}, respectively. We describe herein the preparations and structural characterization of the $Au^{III}-M^{I}$ (M = Cu, Ag, Au) heterovalent or heteronuclear complexes, together with luminescent properties of the mixed-valence $Au^{III}Au^{I}_4$ compound.

Experimental Section

Materials and Reagents. All operations were performed under argon atmosphere using Schlenk techniques. Solvents were dried by standard methods and distilled prior to use. The reagents 3,4-toluenedithiol (H_2tdt), bis(diphenylphospino)methane (dppm), silver hexafluorophosphonate ($AgPF_6$), and $HAuCl_4$ were available commercially (Acros and Alfa Aesar). The compounds $[Cu_2(dppm)_2(MeCN)_2](ClO_4)_2$,[44] $[Ag_2(dppm)_2(MeCN)_2](PF_6)_2$,[45] $[Au_2(dppm)_2](SbF_6)_2$,[46,47] and $[Bu_4N][Au(tdt)_2]$[48] were prepared by the literature procedures.

$[Au^{III}Cu^{I}_8(\mu\text{-dppm})_3(tdt)_5](ClO_4)_{1/2}(SbF_6)_{1/2}$ (1). To a dichloromethane (10 mL) solution of $[Bu^n_4N][Au(tdt)_2]$ (37.4 mg, 0.05 mmol) was added a dichloromethane (10 mL) solution of $[Cu_2(dppm)_2(MeCN)_2](ClO_4)_2$ (117.7 mg, 0.10 mmol). After being stirred at room temperature for 1 day with color changing to dark brown, the solution was filtered to remove a little precipitate. The filtrate was then concentrated in vacuo and chromatographed on a silica gel column. The product was eluted with dichloromethane−acetone (40:1 v/v) as the second band. Metathesis of perchlorate using the eluted solution and a methanol solution of sodium hexafluoroantimonate afforded compound **1** as sheetlike dark brown crystals by diffusion of diethyl ether. Yield: 20%. Anal. Calcd for $C_{110}H_{96}AuCl_{0.50}Cu_8F_3O_2P_6S_{10}Sb_{0.50}\cdot 5/2H_2O$: C, 46.48, H, 3.58. Found: C, 46.42; H, 3.47. IR spectrum (KBr, cm^{-1}): ν 1099 (s, ClO_4), 658 (s, SbF_6). ^1H NMR (DMSO-d_6, ppm): δ 7.78−7.27 (m, 60H, C_6H_5), 7.00−6.06 (m, 15H, $C_6H_3S_2$), 3.54 (m, 6H, PCH_2P), 2.37−2.16 (m, 15H, CH_3). ^{31}P NMR ($CDCl_3$, ppm): δ −5.3 (s), −5.9 (s), −11.0 (s), −12.8 (s), −14.0 (s), and −22.7 (s).

$[Au^{III}_3Ag^{I}_8(\mu\text{-dppm})_4(tdt)_8](PF_6)$ (2). This compound was prepared by the same synthetic procedure as that of **1** using $[Ag_2(dppm)_2(MeCN)_2](PF_6)_2$ instead of $[Cu_2(dppm)_2(MeCN)_2](ClO_4)_2$. Recrystallization of the product by layering diethyl ether onto its dichloromethane−methanol solution gave orange crystals. Yield: 55%. Anal. Calcd for $C_{156}H_{136}F_6P_9S_{16}Ag_8Au_3\cdot 2CH_2Cl_2\cdot CH_3OH\cdot 2H_2O$: C, 41.44; H, 3.24. Found: C, 41.86; H, 3.45. IR spectrum (KBr, cm^{-1}): ν 839 (s, PF_6). ^1H NMR (CD_3CN, ppm): δ 7.78−7.28 (m, 80H, C_6H_5), 6.72−6.57 (m, 24H, $C_6H_3S_2$), 3.97 (s, 8H, PCH_2P), 2.11 (s, 24H, CH_3). ^{31}P NMR (CD_3CN, ppm): δ 7.9 (d, J_{Ag-P} = 476 Hz).

$[Au^{III}Au^{I}_4(\mu\text{-dppm})_4(tdt)_2](SbF_6)_3$ (3). To a dichloromethane (20 mL) solution of $[Bu^n_4N][Au(tdt)_2]$ (37.4 mg, 0.05 mmol) was added $[Au_2(dppm)_2](SbF_6)_2$ (163.4 mg, 0.10 mmol) giving a brown yellow solution. It was stirred at room temperature for 1 day to yield a khaki suspension. The solvent was then removed in vacuo, and the residue was dissolved in 4 mL of acetonitrile to give a mixture that was filtered to afford a yellow solution. Yellow crystals (130 mg) were grown by layering diethyl ether onto the solution. Yield: 73%. Anal. Calcd for $C_{114}H_{100}Au_5F_{18}P_8S_4Sb_3$: C, 38.70; H, 2.85. Found: C, 38.62; H, 2.81. ES-MS (*m*/*z*): 1667 ($[Au_3(dppm)_2(tdt)_2]^+$), 944 ($[M-3(SbF_6)]^{3+}$), 814 ($[Au_5(dppm)_3(tdt)_2)]^{3+}$), 581 ($[Au_2(dppm)_2]^{2+}$). IR spectrum (KBr, cm^{-1}): ν 658 (s, SbF_6). ^1H NMR (DMSO-d_6, ppm): δ 7.87−7.46 (m, 80H, C_6H_5), 6.80−6.58 (m, 6 H, $C_6H_3S_2$), 5.01 (s, 8H, PCH_2P), 2.14 (s, 6H, CH_3). ^{31}P NMR spectrum (CD_3CN, ppm): δ 34.5 (s).

Crystal Structural Determination. Single crystals sealed in capillaries with mother liquors were measured on a Siemens SMART CCD diffractometer by the ω scan technique at room

---

(23) Usón, R.; Laguna, A.; Laguna, M.; Manzano, B. R.; Jones, P. G.; Sheldrick, G. M. *J. Chem. Soc., Dalton Trans.* **1985**, 2417.

(24) Schmidbaur, H.; Hartmann, C.; Reber, G.; Müller, G. *Angew. Chem., Int. Ed. Engl.* **1987**, *26*, 1146.

(25) Jarvis, J. A.; Johnson, A.; Puddephatt, R. J. *J. Chem. Soc., Chem. Commun.* **1973**, 373.

(26) Usón, R.; Laguna, A.; Laguna, M.; Tartón, M. T.; Jones, P. G. *J. Chem. Soc., Chem. Commun.* **1988**, 740.

(27) Castro-Castro, L. M.; Guloy, A. M. *Inorg. Chem.* **2004**, *43*, 4537.

(28) Hollis, L. S.; Lippard, S. J. *J. Am. Chem. Soc.* **1983**, *105*, 4293.

(29) Bennett, M. A.; Hockless, D. C. R.; Rae, A. D.; Welling, L. L.; Willis, A. C. *Organometallics* **2001**, *20*, 79.

(30) Fernández, E. J.; Gimeno, M. C.; Jones, P. G.; Laguna, A.; Laguna, M.; López-de-Luzuriaga, J. M. *Organometallics* **1995**, *14*, 2918.

(31) Raptis, R. G.; Fackler, J. P., Jr. *Inorg. Chem.* **1990**, *29*, 5003.

(32) Raptis, R. G.; Porter, L. C.; Emrich, R. J.; Murray, H. H.; Fackler, J. P., Jr. *Inorg. Chem.* **1990**, *29*, 4408.

(33) Fackler, J. P., Jr.; Trzcinska-Bancroft, B. *Organometallics* **1985**, *4*, 1891.

(34) Mazany, A. M.; Fackler, J. P., Jr. *J. Am. Chem. Soc.* **1984**, *106*, 801.

(35) Blanco, M. C.; Fernández, E. J.; López-de-Luzuriaga, J. M.; Olmos, M. E.; Crespo, O.; Gimeno, M. C.; Laguna, A.; Jones, P. G. *Chem.−Eur. J.* **2000**, *6*, 4116.

(36) Blanco, M. C.; Fernández, E. J.; Jones, P. G.; Laguna, A.; López-de-Luzuriaga, J. M.; Olmos, M. E. *Angew. Chem., Int. Ed.* **1998**, *37*, 3042.

(37) Blanco, M. C.; Fernández, E. J.; Olmos, M. E.; Crespo, O.; Laguna, A.; Jones, P. G. *Organometallics* **2002**, *21*, 2426.

(38) Canales, F.; Canales, S.; Crespo, O.; Gimeno, M. C.; Jones, P. G.; Laguna, A. *Organometallics* **1998**, *17*, 1617.

(39) Coucouvanis, D.; Kanodia, S.; Swenson, D.; Chen, S.-J.; Stüdemann, T.; Baenziger, N. C.; Pedelty, R.; Chu, M. *J. Am. Chem. Soc.* **1993**, *115*, 11271.

(40) Chen, Y.-D.; Zhang, L.-Y.; Shi, L.-X.; Chen, Z.-N. *Inorg. Chem.* **2004**, *43*, 7493.

(41) Chen, Y.-D.; Qin, Y.-H.; Zhang, L.-Y.; Shi, L.-X.; Chen, Z.-N. *Inorg. Chem.* **2004**, *43*, 1197.

(42) Wei, Q.-H.; Zhang, L.-Y.; Yin, G.-Q.; Shi, L.-X.; Chen, Z.-N. *J. Am. Chem. Soc.* **2004**, *126*, 9940.

(43) Wei, Q.-H.; Yin, G.-Q.; Zhang, L.-Y.; Shi, L.-X.; Mao, Z.-W.; Chen, Z.-N. *Inorg. Chem.* **2004**, *43*, 3484.

(44) Diez, J.; Gamasa, M. P.; Gimeno, J.; Tiripicchio, A.; Camellini, M. T. *J. Chem. Soc., Dalton Trans.* **1987**, 1275.

(45) Ho, D. M.; Bau, R. *Inorg. Chem.* **1983**, *22*, 4073.

(46) Lin, I. J. B.; Hwang, J. M.; Feng, D.-F.; Cheng, M. C.; Wang, Y. *Inorg. Chem.* **1994**, *33*, 3467.

(47) Che, C.-M.; Kwong, H.-L.; Poon, C.-K.; Yam, V. W.-W. *J. Chem. Soc., Dalton Trans.* **1990**, 3215.

(48) Mazid, M. A.; Razi, M. T.; Sadler, P. J. *Inorg. Chem.* **1981**, *20*, 2872.

Table 1. Crystallographic Data for Compounds **1**·5/2H_2O, **2**·2CH_2Cl_2·CH_3OH·2H_2O, and **3**

	1·5/2H_2O	**2**·2CH_2Cl_2·CH_3OH· 2H_2O	**3**
empirical formula	$C_{110}H_{101}AuC_{10.5}Cu_8F_3O_{4.5}P_6S_{10}Sb_{0.5}$	$C_{159}H_{148}Ag_8Au_3Cl_4F_6O_3P_9S_{16}$	$C_{114}H_{97}Au_5F_{18}P_8S_4Sb_3$
fw	2842.21	4608.12	3535.00
space group	Pbcn	$C2/c$	$P\bar{1}$
a, Å	16.4017(3)	37.5166(6)	15.716(4)
b, Å	33.8460(5)	24.9903(2)	15.770(3)
c, Å	45.2340(5)	21.4683(4)	26.735(7)
α, deg			81.948(9)
β, deg		90.1890(10)	85.843(9)
γ, deg			64.465(5)
V, Å^3	25 110.8(7)	20 127.5(5)	5919(2)
Z	8	4	2
ρ_{calcd}, g/cm^3	1.504	1.521	1.983
μ, mm^{-1}	2.899	3.276	7.098
radiatn (λ, Å)	0.710 73	0.710 73	0.710 73
temp, K	293(2)	293(2)	293(2)
R1^a(F_o)	0.1219	0.0973	0.0585
wR2^b(F_o^2)	0.2844	0.2234	0.1322
GOF	1.219	1.260	1.095

^{a} $R1 = \Sigma|F_o - F_c|/\Sigma F_o$. ^{b} $wR2 = \Sigma[w(F_o^2 - F_c^2)^2]/\Sigma[w(F_o^2)]^{1/2}$.

temperature using graphite-monochromated Mo Kα ($\lambda = 0.710\ 73$ Å) radiation. Absorption corrections by SADABS were applied to the intensity data. The structures were solved by direct methods, and the heavy atoms were located from an E-map. The remaining non-hydrogen atoms were determined from the successive difference Fourier syntheses. All non-hydrogen atoms were refined anisotropically, and the hydrogen atoms were generated geometrically and refined with isotropic thermal parameters. The structures were refined on F^2 by full-matrix least-squares methods using the SHELXTL-97 program package.[49] The crystallographic data for **1**·5/2H_2O, **2**·2CH_2Cl_2·CH_3OH·2H_2O, and **3** are summarized in Table 1.

For compound **1**·5/2H_2O, the C−C distances (1.380 ± 0.005 Å) in phenyl rings C21−C26, C41−C46, C161−C166, and C191−C196 were fixed in refinement of the structure. The carbon atoms of methyls in tdt exhibit a statistical distribution, where the occupancy factors for C17, C17′, C37, C37′, C47, C47′, C57, and C57′ are 0.50, respectively, whereas those for C27 and C27′ are 0.75 and 0.25, respectively. The poor quality of the crystals led to a high R (0.1219) factor, but the refined structure is reliable and gives reasonable bond parameters. As the reflection data in high 2θ angle are quite bad, only those with $2\theta \leq 45°$ were used for the refinement. The structure of compound **2**·2CH_2Cl_2·CH_3OH·2H_2O was refined by fixing the P−F (1.550 ± 0.005 Å) distances in hexafluorophosphate and the C−Cl (1.765 ± 0.005 Å) lengths in solvate dichloromethane. For compound **3**, one of the gold atoms was located in a statistic distribution with the occupancy factors of 0.90 and 0.10 for Au1 and Au1′, respectively. The Sb−F (1.850 ± 0.005 Å) distances in hexafluoroantimonate were fixed in the refinement.

Physical Measurements. Elemental analyses (C, H) were performed on a Perkin-Elmer model 240C automatic instrument. Electrospray ion mass spectra (ES-MS) were recorded on a Finnigan DECAX-30000 LCQ mass spectrometer using acetonitrile−methanol as mobile phase. UV−vis absorption spectra were measured on a Perkin-Elmer Lambda 25 UV−cis spectrometer. Infrared spectra were recorded on a Magna750 FT-IR spectrophotometer with KBr pellets. ^{1}H and ^{31}P NMR spectra were measured on a Varian UNITY-500 spectrometer with $SiMe_4$ as the internal reference and 85% H_3PO_4 as external standard, respectively. Cyclic voltammograms were run with a potentiostat/galvanostat model 263A in dichloromethane solutions containing 0.1 M $[Bu^n{}_4N][PF_6]$ as supporting electrolyte. Cyclic voltammetry was performed at a scan rate of 100 mV s^{-1}. Platinum and glassy graphite were used as counter and working electrodes, respectively, and the potentials were measured against the Ag/AgCl reference electrode. Emission and excitation spectra were recorded on a Perkin-Elmer LS 55 luminescence spectrometer with a red-sensitive photomultiplier type R928. Emission lifetimes were determined on an Edinburgh Analytical Instrument (F900 fluorescence spectrometer) using an LED laser at 340 nm excitation, and the resulting emission was detected by a thermoelectrically cooled Hamamatsu R3809 photomultiplier tube. The instrument response function at the excitation wavelength was deconvoluted from the luminescence decay, and the decay was fitted using a least-squares method for exponential functions.

Results and Discussion

As shown in Scheme 1, reactions of $[Au^{III}(tdt)_2]^-$ with 2 equiv of $[M^I{}_2(dppm)_2]^{2+}$ gave heterovalent or heteronuclear $Au^{III}Cu^I{}_8$, $Au^{III}{}_3Ag^I{}_8$, and $Au^{III}Au^I{}_4$ complexes when M = Cu^I, Ag^I, and Au^I, respectively. Variation in molar ratios between $[Au^{III}(tdt)_2]^-$ and $[M^I{}_2(dppm)_2]^{2+}$ afforded compounds **1**−**3** in lower yields**.** While formation of the unexpected $Au^{III}Cu^I{}_8$ and $Au^{III}{}_3Ag^I{}_8$ complexes is related to the dissociation and recombination between the two starting metal components, incorporating two binuclear $[Au^I{}_2(dppm)_2]^{2+}$ components with one $[Au^{III}(tdt)_2]^-$ unit gives indeed the desired $Au^{III}Au^I{}_4$ products.

The ^{31}P NMR spectrum of **1** showed six singlets at −5.3, −5.9, −11.0, −12.8, −14.0, and −22.7 ppm, respectively, consistent with the existence of six inequivalent phosphorus atoms in its solid-state structure. In the ^{31}P NMR spectrum of **2**, only one doublet is observed at 7.9 ppm with obvious Ag−P coupling ($J_{Ag-P} = 476$ Hz), indicating that the P donors are unresolved on the NMR time scale. The occurrence of one singlet at 34.5 ppm in the ^{31}P NMR spectrum of **3** also reveals the equivalence of the P donors. It appears that both ^{1}H and ^{31}P NMR spectra of compounds **2** and **3** are consistent with their structures in the solid state.

Perspective views of the coordination cations of **1**−**3** with atom-numbering scheme are depicted in Figures 1−3,

---

(49) Sheldrick, G. M. *SHELXL-97, Program for the Refinement of Crystal Structures*; University of Göttingen: Göttingen, Germany, 1997.

Scheme 1. Synthetic Routes to Compounds **1**−**3**

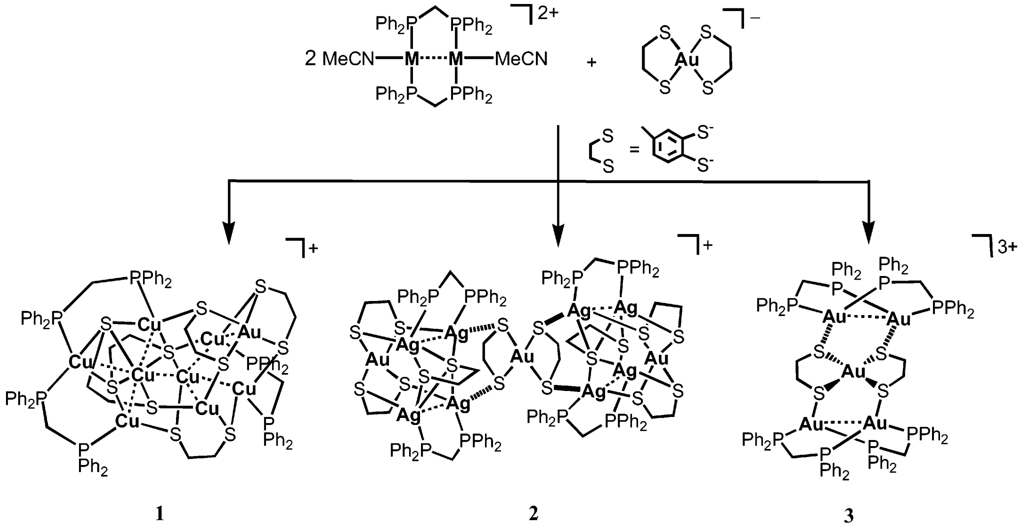

Chart 1

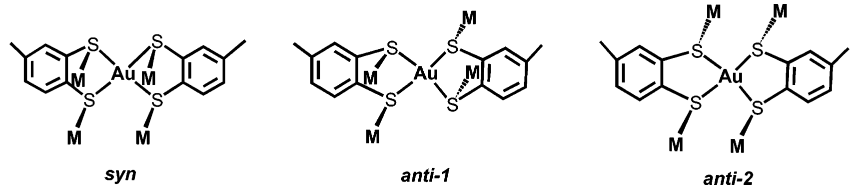

Chart 2

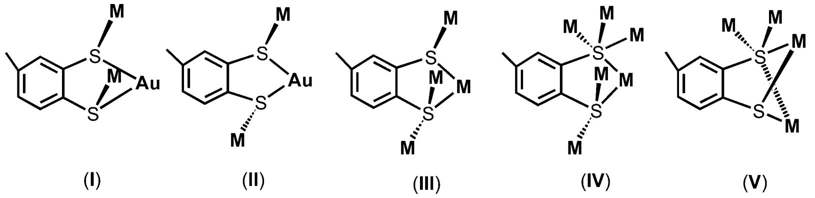

respectively. As shown in Chart 1, the Au(tdt)$_2$ component affords a square-planar S$_4$ chromophore to link four M^{I} ions together by the sulfur donors in three different conformations or orientations. It adopts syn and anti-2 conformations in Au^{III}Cu$^{I}_8$ compound **1** and Au^{III}Au$^{I}_4$ compound **3** (Scheme 1), respectively, whereas both syn and anti-1 conformations are present in Au$^{III}_3$Ag$^{I}_8$ compound **2**. The tdt ligand exhibits five different types of bonding modes as depicted in Chart 2, chelating Au^{III} or M^{I} as well as bridging M^{I} in various orientations and different numbers of Au^{III}−S−M^{I} linkages. It is noteworthy that bonding modes I and II only differ in orientations of the Au^{III}−S−M^{I} linkages, in which the tdt ligand employs two sulfur donors not only to chelate a Au^{III} atom but also to bridge two M^{I} atoms in syn (mode I) or anti (mode II) orientations.[40,41] The Au^{III}−S (2.311(5)−2.374(3) Å) distances of Au(tdt)$_2$ components in compounds **1**−**3** (Table 2) are slightly elongated relative to those (2.299(4)−2.319(4) Å) in the parent compound [Bu$_4$N][Au(tdt)$_2$].[48] This is likely due to formation of the Au^{III}−S−M^{I} linkages in compounds **1**−**3** which reduces electronic density of the sulfur donors and thus weakens the Au^{III}−S bonds. As a general rule,[19,20] it is shown that narrower Au^{III}−S−M^{I} or M^{I}−S−M^{I} angles are always correlated to shorter Au^{III}−M^{I} or M^{I}−M^{I} contacts in compounds **1**−**3**.

The heterononanuclear complex cation [AuCu$_8$(μ-dppm)$_3$(tdt)$_5$]$^+$ of **1** consists of eight Cu^{I} and one Au^{III} atoms linked together by six P donors from three dppm and 10 μ-, μ_3-, or μ_4-S donors from five tdt ligands. Formation of the Au^{III}Cu$^{I}_8$ assembly may be regarded as incorporation of octanuclear [Cu$^{I}_8$(μ-dppm)$_3$(tdt)$_3$]$^{2+}$ with [Au(tdt)$_2$]$^-$ through four Au^{III}−S−Cu^{I} linkages in syn conformation as depicted in Figure 1. The tdt ligand adopts bonding modes I, III, and IV (Chart 2), chelating Au^{III} or Cu^{I} as well as bridging Cu^{I} atoms by the Au^{III}−S−Cu^{I} linkages to afford the Au^{III}Cu$^{I}_8$ cluster. While the linkage between Cu^{I} and Au^{III} centers is through bonding mode I, the tdt ligand adopts modes III and IV to link Cu^{I} centers together. The Au^{III} center is located at an approximately square-planar environment with the chelating tdt S$_4$ chromophore. The Cu^{I} centers, however, display distorted tetrahedral or trigonal-planar geometries. As depicted in Figure 1, Cu1, Cu2, and Cu4 centers are surrounded by PS$_3$, S$_4$, and P$_2$S$_2$ chromophores, respectively, to afford a distorted tetrahedral geometry. Cu3 and Cu7 centers are in approximately trigonal-planar surroundings with S$_3$ chromophores, and the trigonal coordination planes of Cu5, Cu6, and Cu8 centers are built by PS$_2$ donors, respectively. The neighboring Cu^{I}−Cu^{I} separations are in the range 2.700(5)−2.985(5) Å, indicating the presence of

Table 2. Selected Bond Distances (Å) and Angles (deg) of Compounds **1**−**3**

1		**2**		**3**	
Au1−Cu8	3.215(3)	Ag1−Ag2	3.331(2)	Au1−Au2	3.1253(13)
Cu1−Cu2	2.701(5)	Ag3−Ag4	3.258(2)	Au3−Au4	3.1668(9)
Cu2−Cu3	2.805(5)	Au1−S7	2.311(5)	Au1−P2	2.336(3)
Cu2−Cu4	2.727(5)	Au1−S8	2.328(6)	Au1−P4	2.342(3)
Cu2−Cu5	2.702(5)	Au2−S1	2.340(6)	Au2−P1	2.369(2)
Cu3−Cu6	2.984(5)	Au2−S2	2.331(5)	Au2−P3	2.355(2)
Cu3−Cu7	2.742(5)	Au2−S3	2.329(6)	Au2−S4	2.710(3)
Cu3−Cu8	2.961(4)	Au2−S4	2.327(5)	Au3−P6	2.304(3)
Au1−S1	2.328(7)	Ag1−P1	2.448(5)	Au3−P7	2.314(3)
Au1−S2	2.365(8)	Ag1−S2	2.775(6)	Au3−S1	2.837(3)
Au1−S3	2.350(8)	Ag1−S5	2.531(5)	Au4−P5	2.311(3)
Au1−S4	2.347(7)	Ag1−S8	2.771(6)	Au4−P8	2.318(2)
Cu1−P1	2.276(9)	Ag2−P2	2.470(6)	Au4−S3	2.932(3)
Cu1−S3	2.340(8)	Ag2−S1	2.766(6)	Au5−S1	2.342(3)
Cu1−S6	2.417(8)	Ag2−S5	2.893(5)	Au5−S2	2.336(3)
Cu1−S9	2.378(8)	Ag2−S6	2.555(6)	Au5−S3	2.349(3)
Cu2−S5	2.389(8)	Ag3−P4	2.461(6)	Au5−S4	2.374(3)
Cu2−S6	2.601(7)	Ag3−S3	2.744(6)		
Cu2−S9	2.375(9)	Ag3−S5	2.900(5)		
Cu2−S10	2.292(8)	Ag3−S6	2.531(6)		
Cu3−S6	2.254(8)	Ag4−P3	2.466(5)		
Cu3−S7	2.283(8)	Ag4−S4	2.730(5)		
Cu3−S8	2.272(7)	Ag4−S5	2.537(5)		
Cu4−P2	2.299(9)	Ag4−S7	2.838(5)		
Cu4−P3	2.280(9)				
Cu4−S5	2.417(8)				
Cu4−S9	2.443(10)				
Cu5−P4	2.234(7)				
Cu5−S5	2.304(8)				
Cu5−S8	2.254(8)				
Cu6−P6	2.227(8)				
Cu6−S2	2.341(8)				
Cu6−S7	2.234(8)				
Cu7−S4	2.253(8)				
Cu7−S7	2.306(8)				
Cu7−S10	2.201(8)				
Cu8−P5	2.256(8)				
Cu8−S1	2.366(7)				
Cu8−S6	2.311(7)				
Au1−S1−Cu8	86.5(2)	Au2−S2−Ag1	103.7(2)	Au5−S1−Au3	82.39(9)
Cu6−S2−Au1	100.6(3)	Au2−S1−Ag2	86.48(17)	Au1−S2−Au5	84.90(9)
Cu1−S3−Au1	110.4(3)	Au2−S3−Ag3	87.11(16)	Au5−S3−Au4	103.98(10)
Cu7−S4−Au1	94.4(3)	Au2−S4−Ag4	100.17(19)	Au5−S4−Au2	106.52(10)
Cu5−S5−Cu2	70.3(2)	Ag1−S5−Ag4	116.84(18)		
Cu5−S5−Cu4	113.2(3)	Ag1−S5−Ag2	75.43(13)		
Cu2−S5−Cu4	69.1(2)	Ag4−S5−Ag2	139.5(2)		
Cu3−S6−Cu8	80.9(2)	Ag1−S5−Ag3	143.0(2)		
Cu3−S6−Cu1	122.6(3)	Ag4−S5−Ag3	73.30(13)		
Cu8−S6−Cu1	123.8(3)	Ag2−S5−Ag3	76.03(12)		
Cu3−S6−Cu2	70.2(2)	Ag3−S6−Ag2	89.09(19)		
Cu8−S6−Cu2	147.3(3)	Au1−S7−Ag4	105.7(2)		
Cu1−S6−Cu2	65.02(19)	Au1−S8−Ag1	99.4(2)		
Cu6−S7−Cu3	82.7(3)				
Cu3−S7−Cu7	73.4(3)				
Cu6−S7−Cu7	122.2(3)				
Cu5−S8−Cu3	88.7(3)				
Cu2−S9−Cu1	69.3(2)				
Cu2−S9−Cu4	68.9(3)				
Cu1−S9−Cu4	104.8(3)				
Cu7−S10−Cu2	86.1(3)				

strong copper(I)−copper(I) contacts.[1] The shortest Cu^{I}−Au^{III} distances are 3.216(4) and 3.376(4) Å, implying the presence of a Cu^{I}−Au^{III} interaction, although weak.[35,36,39] Four Au^{III}−S−M^{I} angles are 86.5(2), 94.4(3), 100.6(3), and 110.4(3)°, and the corresponding Cu^{I}···Au^{III} distances are 3.216(4), 3.376(4), 3.622(4), and 3.851(4) Å, respectively. Obviously, the narrowest Au−S−Cu angle (86.5(2)°) corresponds to the shortest Cu^{I}−Au^{III} distance (3.216(4) Å).[19,20] In the same way, the shortest (2.701(5) Å) and longest (2.985(5)°) Cu^{I}−Cu^{I} distances correlate with the narrowest (65.02(19)°) and widest (122.6(3)°) Cu−S−Cu angles, respectively. It is interesting that the Cu1, Cu3, Cu4, and Cu5 atoms form a quadrangle with the Cu2 atom located 0.602 Å above this plane, whereas Cu2, Cu6, Cu7, and Cu8 atoms afford another quadrangle with Cu3 and Au1 atoms situated 1.147 and 2.652 Å above and below this plane, respectively.

As shown in Figure 2, the heteroundecanuclear $\mathrm{Au^{III}_{3}Ag^{I}_{8}}$ complex cation of **2** exhibits a centrosymmetric structure with

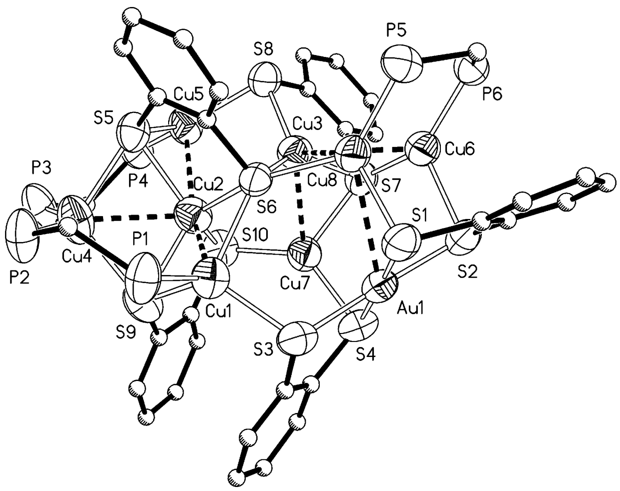

Figure 1. ORTEP drawing of the complex cation of **1** with atom-labeling scheme (30% thermal ellipsoids). Phenyl rings on the phosphorus atoms are omitted for clarity.

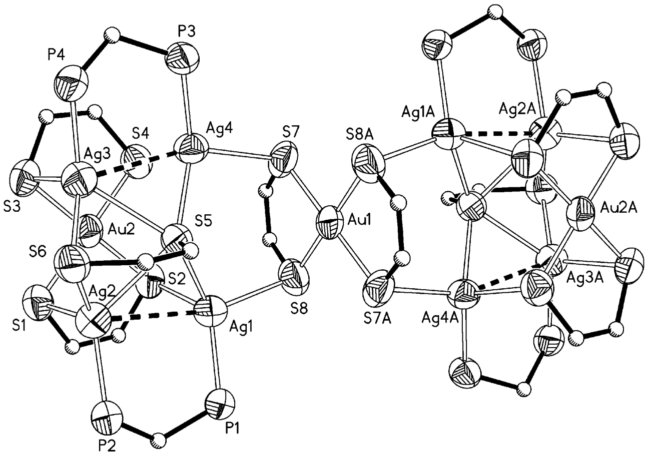

Figure 2. ORTEP drawing of the complex cation of **2** with atom-labeling scheme (30% thermal ellipsoids). Phenyl rings on the phosphorus atoms are omitted for clarity.

the Au1 atom situated at the inversion center. The Au$^{III}_{3}$-Ag$^{I}_{8}$ assembly may be considered as resulting from the incorporation of three Au(tdt)$_2$ components with two Ag$_4$-(μ-dppm)$_2$(tdt) fragments through Au^{III}−S−Ag^{I} linkages. Of the three Au(tdt)$_2$ components, the Au^{III}−S−Ag^{I} linkage for the Au1 atom adopts an anti-1 orientation (Chart 1), whereas those for Au2 and Au3 atoms display syn conformation. The coordination plane of Au(tdt)$_2$ in the middle (Au1) forms a dihedral angle of 80.6° with the plane of Au(tdt)$_2$ at each sides (Au2 and Au2A). The tdt ligand adopts modes I and V (Chart 2) to link Au^{III}−Ag^{I} and Ag^{I}−Ag^{I}, respectively. While the Au^{III} atoms are surrounded by S$_4$ donors arranged in a square-planar geometry, the Ag^{I} atoms are located in distorted tetrahedral environments composed of PS$_3$ chromophores. The Ag$^{I}\cdots$Ag^{I} distances are in the range 3.259(2)−3.322(2) Å, whereas the shortest Au$^{III}\cdots$Ag^{I} distances are 3.507(2) and 3.507(3) Å, respectively, suggesting the presence of weak Ag^{I}−Ag^{I} and Au^{III}-Ag^{I} contacts.[35−38]

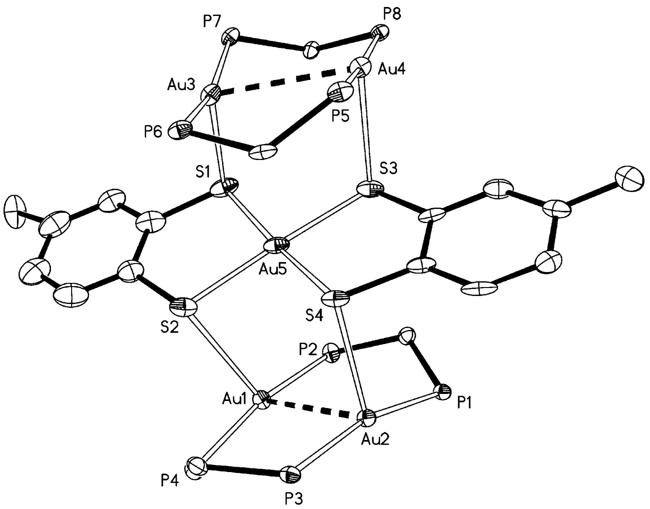

Figure 3. ORTEP drawing of the complex cation of **3** with atom-labeling scheme (30% thermal ellipsoids). Phenyl rings on the phosphorus atoms are omitted for clarity.

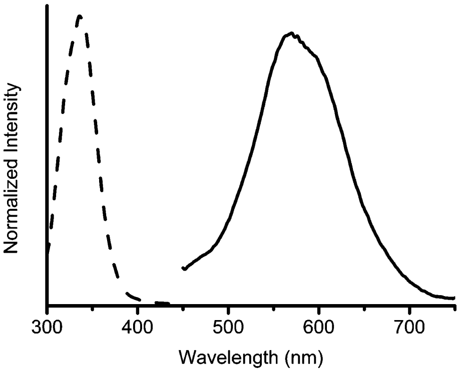

Figure 4. Excitation (dashed line) and emission (solid line) spectra of compound **3** in degassed acetonitrile solution at 298 K.

The complex cation of **3** consists of one [Au(tdt)$_2$]$^{-}$ and two [Au$_2$(μ-dppm)$_2$]$^{2+}$ components linked together through Au^{III}−S−Au^{I} linkages in an anti-2 (Chart 1) conformation as shown in Figure 3. The tdt ligand adopts bonding mode II (Chart 2) in an anti orientation to chelate the Au^{III} atom as well as to bridge the Au^{I} atoms by the sulfur donors. The coordination plane of the Au^{III} (Au5) atom forms dihedral angles of 77.7 and 83.4° with the planes defined by Au1Au2S2S4 and Au3Au4S1S3, respectively. The Au^{III} atom is located at approximately square-planar geometry composed of S$_4$ donors. The Au^{I} atom, however, is surrounded by P$_2$S donors with "T" geometry. The Au^{III}−S (2.336(3)−2.374(3) Å) distances are much shorter than those of Au^{I}−S (2.710(3)−2.932(3) Å). The Au^{I}−Au^{I} (3.1253(13) and 3.1668(9) Å) distances imply the presence of moderate aurophilicity.[1,2] The Au$^{I}\cdots$Au^{III} distances, however, are much longer (3.431−4.177 Å). Again, the narrowest (82.39(9)°) and widest (106.52(10)°) Au^{I}−S−Au^{III} angles correspond to the shortest (3.431 Å) and longest (4.177 Å) Au$^{I}\cdots$Au^{III} separations, respectively.

The redox behavior of compounds **1**−**3** in dichloromethane solution containing 0.10 M [Bu$^{n}_{4}$N][PF$_6$] was investigated by cyclic voltammetry (CV). The parent compound [Bu$_4$N][Au(tdt)$_2$] exhibits two quasi-reversible redox waves at −0.09 and −2.18 V versus Fc^{+}/Fc. According to the assignment suggested by Ray and Wieghardt,[50] the first process is due

---

(50) Ray K.; Weyhermüller, T.; Goossens, A.; Crajè, M. W. J.; Wieghardt, K. *Inorg. Chem.* **2003**, *42*, 4082.

Table 3. Absorption and Emission Data of Compounds 1-3

compd	medium	λ_{abs}/nm (ϵ/dm^{3}mol^{-}1 cm^{-}1)	λ_{em}/nm (τ_{em}/μs) at 298 K	λ_{em}/nm at 77 K
1	MeCN	243 (44 800), 253 (43 600), 290 (26 920), 327 (9590)		
2	MeCN	210 (44 920), 233 (39 200), 260 (30 700), 313 (10 030)		
3	solid		555 (3.1)	536
	MeCN	244 (94 030), 290 (76 800), 328 (16 750), 439 (1100)	570 (1.5)	545

to tdt ligand-centered one-electron oxidation, whereas the second likely arises from metal-centered one-electron reduction. For compound **1,** the reversible oxidation and reduction waves occur at 0.16 and −1.08 V, respectively. Significant anodic shift for the metal-centered reduction in compound **1** relative to that of the parent compound [Bu_4N][Au($tdt)_2$] may be due to formation the $Au^{III}Cu^{I}_8$ cluster structure. In contrast with the reversible redox behavior of compound **1**, compound **2** exhibits an irreversible ligand oxidation wave at −0.01 V and an irreversible metal-centered reduction wave at −1.57 V. The corresponding redox processes for compound **3** were observed at 0.11 and −1.51 V as irreversible redox waves, respectively.

Electronic absorption and emission data for compounds **1**−**3** are listed in Table 3. The UV−vis absorption spectra of compounds **1**−**3** in acetonitrile solutions are dominated by ligand-centered bands in the ultraviolet region. Shoulders appear at ca. 310−330 nm with an absorption tail extending to 450 nm for compound **1** and **2**. Compound **3** exhibits a weak low-energy band at 439 nm (ϵ = 1100 dm^3 mol^{-1} cm^{-1}), possibly originating from metal-perturbed transition of the ligands.

Compounds **1** and **2** are nonemissive whether at room temperature or at 77 K. Compound **3**, however, shows luminescence in the solid state and in acetonitrile solution. Excitation and emission spectra of compound **3** in acetonitrile solution are shown in Figure 4. With excitation at $\lambda_{ex} > 300$ nm, the emissions occur at 555 nm in the solid state and at 570 nm in degassed acetonitrile solution at room temperature. The lifetimes in solid state and in degassed acetonitrile solution at 298 K are 3.1 and 1.5 μs, respectively, suggestive of spin-forbidden character with the triplet excited states.

King and Fackler have demonstrated that the compound [Au(dppm)]$_2$(BF_4)$_2$ shows an intense emission at 593 nm with a long excited-state lifetime ($\tau_{em} = 21$ μs) in fluid acetonitrile solution, and the Au^{I}_2 emissive state appears to be $^3A_u(\sigma^*)$-(σ) in nature.[51] It has been suggested that changing the separation between the two Au^I centers might be expected to change the energy gap between σ^*(s, d_{z^2}) and $\sigma(p_z)$.[52] Compound **3** is composed of one [Au(tdt)$_2$]$^-$ and two [Au_2-(μ-dppm)$_2$]$^{2+}$ components incorporating together through the $Au^{III}-S-Au^I$ linkages. Because of the nonemissive feature for the chromophore Au^{III}(tdt)$_2$, the photoluminescence in compound **3** should originate from the chromophore Au_2-(μ-dppm)$_2$ and/or the $Au^{III}-S-Au^I$ linkages. Compared with that of the precursor compound [Au(dppm)]$_2$(BF_4)$_2$ (λ_{em} = 593 nm), the emission of compound **3** (λ_{em} = 570 nm) in acetonitrile solution shows an obvious shift to higher energy. This is probably elucidated by the elongated Au^I-Au^I separation in compound **3** (3.1253(13) and 3.1668(9) Å) relative to that in [Au(dppm)]$_2$(BF_4)$_2$ (2.931(1) Å), thus increasing the energy gap between σ^*(s, d_{z^2}) and $\sigma(p_z)$ and inducing an obvious blue shift. However, the contribution from S → Au^I ^{3}LMCT or dithiolate ligand to metal (tdt → Au^I) ^{3}LMCT transition[6,7,53−58] cannot be excluded at this stage.

Conclusions

Three heterovalent or heteronuclear $Au^{III}-M^I$ (M = Cu, Ag, Au) cluster complexes were prepared by incorporation of [Au^{III}(tdt)$_2$]$^-$ with M^I_2(dppm)$_2$. Structural characterization of the $Au^{III}Cu^I_8$, $Au^{III}_3Ag^I_6$, and $Au^{III}Au^I_4$ cluster complexes was accomplished, revealing that the dithiolate tdt can afford versatile coordination modes and bonding orientations to give rich structural topology of the $Au^{III}-M^I$ cluster complexes. The rather short $Au^{III}-M^I$ distance suggests the presence of weak $Au^{III}-M^I$ contacts in $Au^{III}Cu^I_8$, $Au^{III}_3Ag^I_6$, and Au^{III}-Au^I_4 cluster complexes. In contrast with nonemissive properties for compounds **1** and **2**, $Au^{III}Au^I_4$ compound **3** shows solid-state and fluid solution luminescence with lifetimes in the microsecond range.

Acknowledgment. This work was supported by the NSFC (Grants 20273074, 20490210, and 90401005), NSF of Fujian Province (Grants E0420002 and E0310029), the fund from the Chinese Academy of Sciences, and the National Basic Research Program (Grant 001CB108906) from the Ministry of Sciences and Technology of China.

Supporting Information Available: X-ray crystallographic files in CIF format for the structure determinations of compounds **1**·5/2H_2O, **2**·2CH_2Cl_2·CH_3OH·2H_2O, and **3**. This material is available free of charge via the Internet at http://pubs.acs.org.

IC050542N

---

(51) King, C, Wang, J.-C., Khan, M. N. I.; Fackler, J. P., Jr. *Inorg. Chem.* **1989**, *28*, 2145.

(52) Mann, K. R.; Thich, J. A.; Bell, R. A.; Coyle, C. L.; Gray, H. B. *Inorg. Chem.* **1980**, *19*, 2462.

(53) Tang, S. S.; Chang, C.-P.; Lin, I. J. B.; Liou, L.-S.; Wang, J.-C. *Inorg. Chem*. **1997**, *36*, 2294.

(54) Mohamed, A. A.; Kani, I.; Ramirez, A. O.; Fackler, J. P., Jr. *Inorg. Chem.* **2004**, *43*, 3833.

(55) Maspero, A.; Kani, I.; Mohamed, A. A.; Omary, M. A.; Staples, R. J.; Fackler, J. P., Jr. *Inorg. Chem.* **2003**, *42*, 5311.

(56) van Zyl, W. E.; Lopez-de-Luzuriaga, J. M.; Mohamed, A. A.; Staples, R. J.; Fackler, J. P., Jr. *Inorg. Chem.* **2002**, *41*, 4579.

(57) Yam, V. W. W.; Li, C. K.; Chan, C. L. *Angew. Chem., Int. Ed.* **1998**, *37*, 2857.

(58) Tzeng, B.-C.; Yeh, H.-T.; Huang, Y.-C.; Chao, H.-Y.; Lee, G.-H.; Peng, S.-M. *Inorg. Chem.* **2003**, *42*, 6008.